Spectroscopic considerations on DIAL measurement of carbon dioxide in volcanic emissions

L. FIORANI[a], W.R. SALEH[b], M. BURTON[c], A. PUIU[a], M. QUEIßER[c]
[a]*UTAPRAD-DIM, ENEA, Via Enrico Fermi 45, 00044 Frascati, Italy*
[b]*Physics Department, College of Science, University of Baghdad, Baghdad, Iraq*
[c]*Istituto Nazionale di Geofisica e Vulcanologia, Via della Faggiola 32, 56126 Pisa, Italy*

The true magnitude of CO_2 emissions from volcanic activity is poorly constrained, limiting our understanding of the natural carbon cycle. CO_2-sensitive lidars could be used to measure the distribution of CO_2 in a volcanic plume, thereby allowing volcanic CO_2 fluxes to be measured directly. The recently-begun ERC research project CO2VOLC aims to produce such an instrument based on the differential absorption lidar (DIAL) technique. In this paper we investigate the ON and OFF wavelengths which offer optimal CO_2 detection and identify the spectral requirements of the lidar transmitter, in the context of commercially available solid-state laser sources.

(Received January 22, 2013; accepted April 11, 2013)

Keywords: Remote sensing, Lidar, DIAL, Atmospheric CO_2, Volcanic emission

1. Introduction

Since the late nineteenth century, global atmospheric carbon dioxide has progressively increased. Artificially produced CO_2 from synthetic sources is considered the most significant of all greenhouse gases [1]: increasing CO_2 concentration in the atmosphere over the last century has been linked to climate change, and future trends of CO_2 will likely be of critical importance to management of carbon emissions and sequestration. For this reason, improved capability for measuring CO_2 concentration has been called for, especially active remote sensing. Studies have indicated that a precision of CO_2 concentration measurement of 0.5% or smaller from a remote sensor is a goal for studies of the global carbon cycle [2].

Volcanoes represent one of the natural processes in the earth's system, which add carbon dioxide to the atmosphere. The global volcanic emission rate has been only approximated, resulting in 34 ± 24 Mt y^{-1}; the high uncertainty is primarily due to the unavailability of long-term measurements for most of the volcanoes and the highly variable nature of volcanic plumes in the eruption processes. Aircraft instruments can measure vertical CO_2 profiles up to an altitude of 10 km but cannot perform continuous measurements. Therefore ground-based laser sensors are attractive methods for obtaining vertical CO_2 profiles.

In addition to quantification on the volcanic contribution to greenhouse gases, the composition of volcanic plumes gives information on the processes inside volcanos and on the possible transition from quiescence to eruption. This explains the interest of geophysicists in laser techniques of gas detection. In particular, they are interested in the lidar (light detection and ranging) [3] measurement of carbon dioxide in volcanic plumes [4] because it could offer high-frequency remote sensing of volcanic gases. Elastic lidar and DIAL (differential absorption lidar) [3] have been used in the past to determine aerosol load [5], SO_2 concentration [6] and water vapor flux [7] in volcanic plumes.

2. DIAL measurement

A lidar is essentially an optical radar composed of a transmitter (laser) and a receiver (telescope). Its principle of operation is illustrated in Fig. 1: the backscatterers (molecules and aerosols) at the distance R from the system send back part of the laser pulse toward A, active surface of the telescope. Consequently, the analysis of the detected signal as a function of t, time interval between emission and detection, allows one to study the optical properties of the atmosphere along the beam, since the simple relation between t and R is given by:

$$R = \frac{ct}{2}, \tag{1}$$

where c is the speed of light.

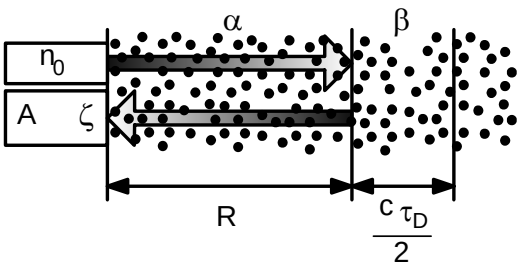

Fig. 1. Lidar principle of operation. The points represent generic atmospheric scatterers (molecules and aerosols).

The photons detected within τ_D, detector response time, are backscattered from the layer delimited by the distances R and $R+c\tau_D/2$. Their number n is proportional to the thickness $c\tau_D/2$ and to the backscattering coefficient β of the involved air volume. Furthermore, in its round trip, the original pulse consisting of n_0 photons is attenuated by the atmosphere. This phenomenon is quantified by the extinction coefficient α. Moreover, n is proportional to the solid angle A/R^2 and the efficiency ζ of the detection system.

On the basis of the preceding discussion, the lidar equation can be written:

$$n(R,\lambda) = n_0(\lambda)\zeta(\lambda)\frac{A}{R^2}\beta(R,\lambda)\frac{c\tau_D}{2}\exp\left[-2\int_0^R \alpha(R',\lambda)dR'\right] \tag{2}$$

Laser remote sensing can be used to measure the concentration of atmospheric gases by DIAL. This system is based on the detection of the backscattered photons from laser pulses transmitted to the atmosphere at two different wavelengths. At one wavelength (λ_{OFF}), the light is almost only scattered by air molecules and aerosols, whereas at the other one (λ_{ON}), it is also absorbed by the gas under study. The difference between the two recorded signals is thus related to the pollutant concentration. More precisely, on the basis of equation (2), the DIAL equation can be derived:

$$C(R) = \frac{1}{2\left[\sigma(\lambda_{ON}) - \sigma(\lambda_{OFF})\right]} \times$$
$$\times\left\{\frac{d}{dR}\ln\left[\frac{n(R,\lambda_{OFF})}{n(R,\lambda_{ON})}\right] - \frac{d}{dR}\ln\left[\frac{\beta(R,\lambda_{OFF})}{\beta(R,\lambda_{ON})}\right] - 2\left[\alpha(R,\lambda_{ON}) - \alpha(R,\lambda_{OFF})\right]\right\}, \tag{3}$$

where C(R) and $\sigma(\lambda)$ are, respectively, the concentration and the absorption cross-section of the gas molecule. If λ_{OFF} and λ_{ON} are close enough, as in the case of CO_2 measurement, equation (3) gets simpler:

$$C(R) = \frac{1}{2\left[\sigma(\lambda_{ON}) - \sigma(\lambda_{OFF})\right]}\frac{d}{dR}\ln\left[\frac{n(R,\lambda_{OFF})}{n(R,\lambda_{ON})}\right] \tag{4}$$

The DIAL principle of operation is illustrated in Fig. 2.

The lidar has been widely applied to atmospheric studies because of its advantages with respect to usual techniques: remote sensing (the investigated air parcel can be up to many kilometers far from the experimental system); continuous retrieval of aerosols load, wind speed and trace gases concentration profile in a considerable range, and with a good spatio-temporal resolution; probe-less measurement, thus eliminating the unwanted possibility of sample modification; integrated-path determination, less sensitive to local effects; multi-gas detection if the laser source is tunable; sweeping capability of the complete hemisphere, thus allowing to accurately follow the physico-chemical dynamics of the atmosphere.

Carbon dioxide absorbs in the 15, 4.2, 2.05 and 1.6 μm bands (in order of decreasing strength) [8]. Unfortunately, in the first two bands viable lasers are not available and atmospheric backscattering is rather low, so the 2.05 and 1.6 μm bands have been suggested [9] for its detection. Nevertheless, the DIAL measurement of CO_2 remains a difficult task because the absorption lines are narrow and weak [10].

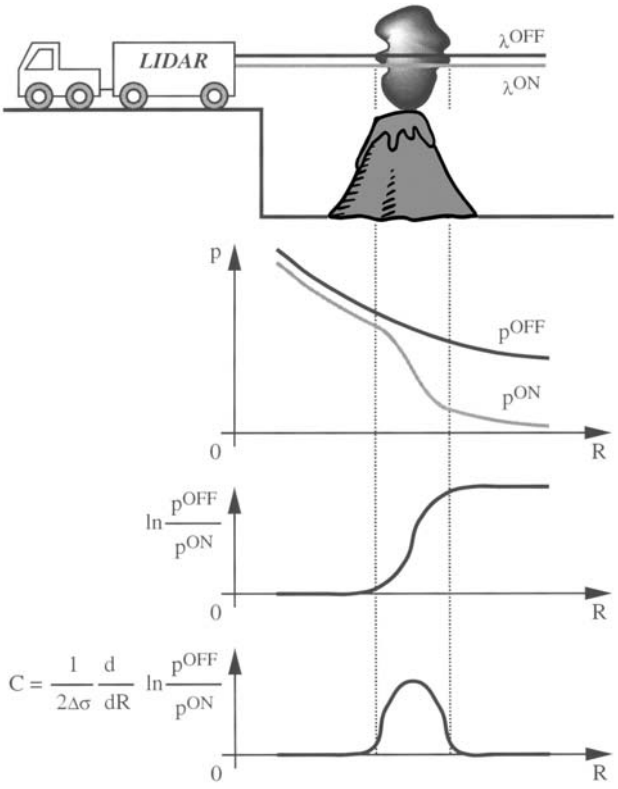

Fig. 2. DIAL principle of operation. The figure does not represent the actual geometry of the experiment.

For all these reasons, a powerful, tunable and narrow-linewidth laser source is highly desirable. Laser technology is a rapidly evolving field. Dye lasers of new conception and OPOs (optical parametric oscillators) are now available as tunable sources in spectroscopic researches thanks to the relevant advantage of narrow linewidth. Nevertheless, up to now, all these sources have been mainly employed in the laboratory because of their relative complexity and fragility. Recently, some narrow-linewidth sources characterized by computer controlled alignment and sealed housing have been developed, making thus possible their deployment in field measurement campaigns. Fiber lasers are also a possible choice. They are more robust and small but have a very limited tunability: the lidar transmitter could contain two of them, the first one tuned at λ_{OFF} and the second one tuned at λ_{ON}.

Recently, holmium-thulium lasers have been employed for DIAL measurements of atmospheric CO_2 for

climatic studies [11, 2]. Although these sources are attractive for their high energy and narrow linewidth, they have two major drawbacks:

1. their range of tunability is very narrow (few tenths of nm) if compared with that of dye lasers and OPOs (about 1 μm), thus allowing the measurement of only carbon dioxide (and not necessarily with the best line that could be out of the tunability interval);
2. they are very complex system, not ready for the market and hardly suitable to field applications.

Thanks to their wide range of tunability from UV (ultraviolet) to near IR (infrared) and the occurrence of many absorption lines in these spectroscopic regions, dye lasers and OPOs will make possible to measure not only CO_2, but many other species relevant to volcanic phenomena and atmospheric chemistry.

Another advantage of dye lasers and OPOs is that they are pumped by Nd:YAG lasers. A frequency tripled Nd:YAG laser has already been employed for Raman lidar measurement of CO_2 in the atmosphere [13], thus giving another string to our bow, although the absolute calibration of Raman lidar remains a difficult task.

The lidar will be positioned below the volcanic plume that will be probed with the laser beam. With such configuration, and scanning the plume in a vertical plane roughly perpendicular to the plume axis, the CO_2 concentrations outside and inside the volcanic plume will be measured. In practice, the lidar will be aimed directing its optical axis by means of a plain mirror. These measurements, once integrated over the whole cross-sectional area of the plume, and upon scaling to the plume transport rate (as derived from the wind speed at the plume altitude), will allow the retrieval of the CO_2 flux.

As we have seen, the lidar return is linked to the optical properties of the atmosphere along the laser beam. In general, the extinction and backscattering coefficient are determined mainly by the aerosols load. This means that the lidar will not only measure gas concentrations but also aerosol loads.

The system could also be used for the measurement of wind speed, thanks to the ability of steering the optics in different directions. According to equation (2), the number of photons backscattered by the atmosphere at a given distance from the instrument is proportional to the backscattering coefficient. This factor is a function of the density of aerosols responsible for the light scattering. Any change in its spatio-temporal distribution during a data acquisition will lead therefore to variations in the lidar returns from one laser shot to another. In particular, a wind flow along the beam axis will be detected from the transport of the spatial inhomogeneities of β along the optical path.

3. Lidar measurement of carbon dioxide: state-of-the-art

The 26th International Laser Radar Conference, held in Porto Heli, Greece, from June 25th to 29th, 2012, has been a real mine of useful information. The world leading experts of lidar measurement of carbon dioxide in the atmosphere were present and from oral and poster presentations, preliminary documents and informal discussions a clear picture of this topic emerged.

First of all, lidar measurement of carbon dioxide in the atmosphere is a challenge. The application of this technique in volcanic plumes will encounter an important difference, i.e. a heavier aerosol load that, on the one hand will increase the lidar signal, on the other hand could prevent the laser beam from penetrating into the plume.

Secondly, many measurements are path integrated and even use a hard target. In our case path integration could be performed summing the output of many ADC (analog-to-digital converter) channels and the hard target could be the flank of the volcano.

As already pointed out, the laser linewidth has to be narrow. Ideally, the source should be single longitudinal mode or, at least, mode hopping should be under control. The actual laser wavelength could be controlled by a wavemeter or a cell filled with carbon dioxide.

As far as detector are concerned, at 1.6 μm PDs (photodiodes), APDs (avalanche photodiodes) and PMTs (photomultiplier tubes) are available, while at 2.05 μm only PDs can be found, although APDs are under development at CEA (Commissariat à l'Energie Atomique), France. APDs are more user-friendly than PMTs and their SNR (signal-to-noise ratio) can be one order of magnitude higher than that of PDs. Using PDs could mean that one has to use a more sophisticated detection, such as coherent detection, due to their relatively low SNR. In conclusion, the 1.6 um region has the advantage that there are efficient direct detection systems widely available, such as PMT with high gain and APD with low electronic noise.

As we have just mentioned, two detection modes are possible, coherent and direct. The first one is more sensitive but has some drawbacks: it is more complex, the telescope cannot exceed the size of 3-4 speckles (i.e about 10 cm), only aerosol backscattering is observed (simply because molecular backscattering has a larger linewidth than the observed one) and it sensitive to Doppler shift.

The main groups working in DIAL measurement of carbon dioxide in the atmosphere are DLR (Germany National Research Center for Aeronautics and Space), EP (École Polytechnique, France), JAXA (Japan Aerospace Exploration Agency), NASA (US National Aeronautics and Space Administration), NICT (Japan National Institute of Information and Communication technology) and TMU (Tokyo Metropolitan University, Japan). The main specifications of their systems are listed in Table 1.

Table 1. Main specifications of DIAL systems for CO_2 measurements in the atmosphere. FOV (field of view). OPG (optical parametric generator). OPA (optical parametric amplifier).

Group	Measurement	Target	Source	λ_{ON} [nm]	λ_{OFF} [nm]	Linewidth	Energy or Power	Repetition rate [Hz]	Pulse duration [ns]	Beam divergence [mrad]	Detection	Telescope diameter [mm]	Telescope FOV [mrad]	Detector	Digitizatio
DLR, Germany	Integrated path	Hard	OPO	1572.024	1572.108	30 MHz	30 mJ	10 (ON & OFF)	25		Direct	200 60	3.3	PIN PD (with 200-mm telescope) ADP (with 60-mm telescope)	
EP, France	Range resolved	Aerosol	Ho:YLF pumped by Tm fiber laser	2050.97	2051.1	15 MHz	3 mJ	1 kHz (ON & OFF)	100		Coherent	100		InGaAs	14 bit 400 MS/s
JAXA, Japan	Range resolved	Aerosol	Fiber laser	1572.992	1573.193	5 fm	1 W	cw chirped			Coherent	110	0.4		
NASA, US	Integrated path	Hard	Tm,Ho:YLF	2051.016	2051.25		80 mJ	10 (ON & OFF)	100	0.1	Direct	400	0.25	0.3 mm InGaAs PIN	10 bit 100 MS/s
NASA, US	Integrated path	Hard	Fiber laser	1571.111	1571.061 or 1571.161	5 MHz	5 W	cw			Coherent				
NICT, Japan	Integrated path	Aerosol or hard	Tm,Ho:YLF	2051.004 ÷ 2051.060	2051.25		80m J	30	140		Coherent	100		InGaAs	8 bit 500 MS/s
TMU, Japan	Integrated path and range resolved	Aerosol or hard	OPG/OPA	1572.992	1573.137		20 mJ	250 (ON & OFF)			Direct	200 & 600		PMT	

4. Spectroscopic considerations

As seen from the argumentation in the introduction, the promising spectral regions left for DIAL are those around 1.6 and 2.05 μm (Figg. 1-2), where the CO_2 absorption coefficient is larger than the H_2O absorption coefficient (the absorption of other atmospheric molecules is negligible). Zooms of Figg. 3-4 in the spectral regions around 1.6 and 2.05 μm are provided in Figs. 5-8.

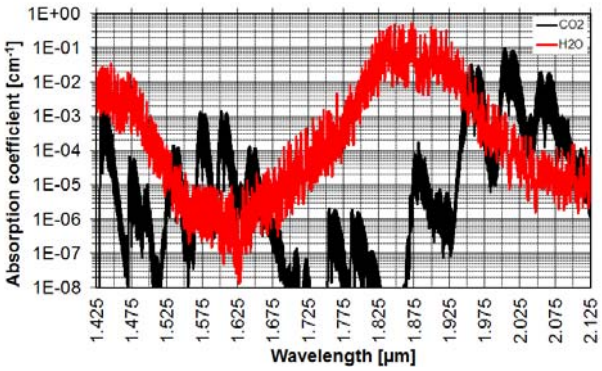

Fig. 3. Absorption coefficient of CO_2 and H_2O (1 atm, 296 K) from 1.425 to 2.125 μm [10].

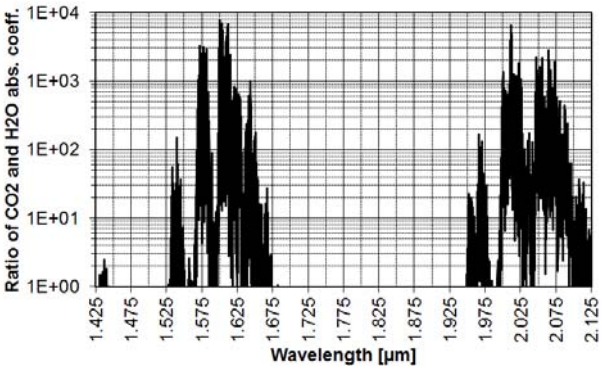

Fig. 4. Ratio between the absorption coefficients of CO_2 and H_2O (1 atm, 296 K) from 1.425 to 2.125 μm [10].

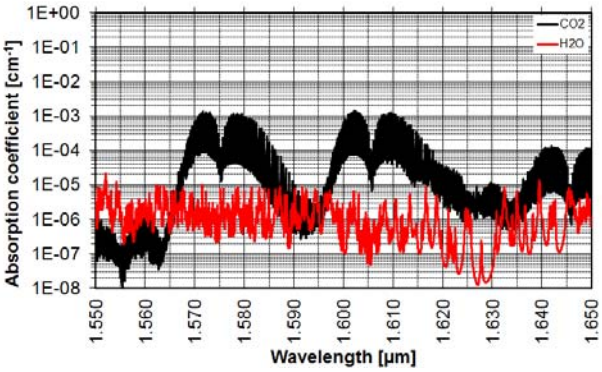

Fig. 5. Absorption coefficient of CO_2 and H_2O (1 atm, 296 K) from 1.55 to 1.65 μm [10].

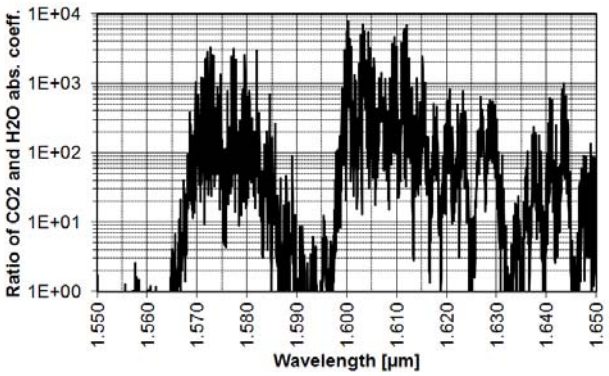

Fig. 6. Ratio between the absorption coefficients of CO_2 and H_2O (1 atm, 296 K) from 1.55 to 1.65 μm [10].

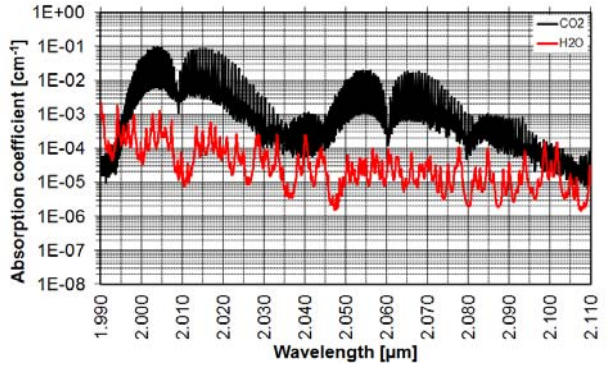

Fig. 7. Absorption coefficient of CO_2 and H_2O (1 atm, 296 K) from 1.99 to 2.11 μm [10].

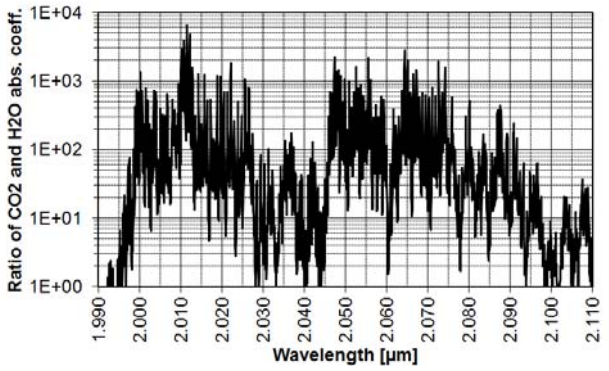

Fig. 8. Ratio between the absorption coefficients of CO_2 and H_2O (1 atm, 296 K) from 1.99 to 2.11 μm [10].

The more promising five spectral windows are: 1570-1585 nm, 1600-1615 nm, 2005-2020 nm, 2045-2060 nm and 2060-2075 nm (Figs. 9-18).

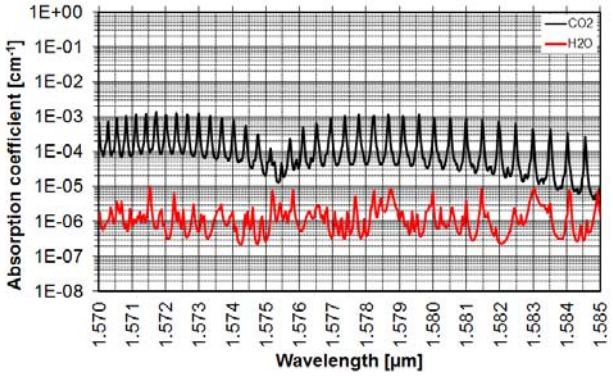

Fig. 9. Absorption coefficient of CO_2 and H_2O (1 atm, 296 K) from 1570 to 1585 nm [10].

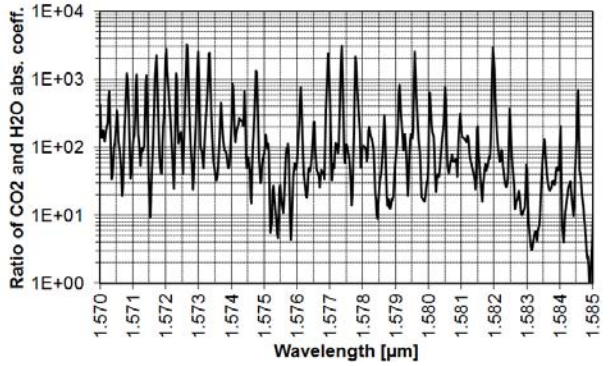

Fig. 10 . Ratio between the absorption coefficients of CO_2 and H_2O (1 atm, 296 K) from 1570 to 1585 nm [10].

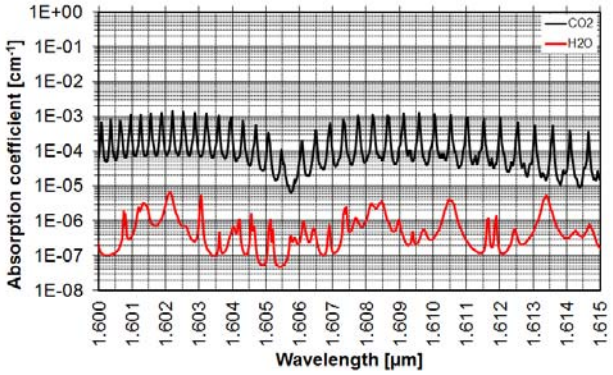

Fig. 11. Absorption coefficient of CO_2 and H_2O (1 atm, 296 K) from 1600 to 1615 nm [10].

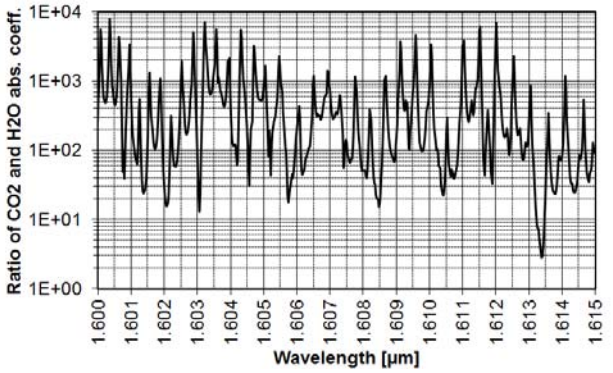

Fig. 12. Ratio between the absorption coefficients of CO_2 and H_2O (1 atm, 296 K) from 1600 to 1615 nm [10].

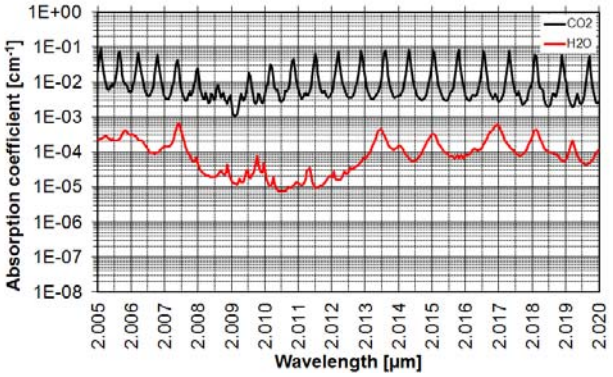

Fig. 13. Absorption coefficient of CO_2 and H_2O (1 atm, 296 K) from 2005 to 2020 nm [10].

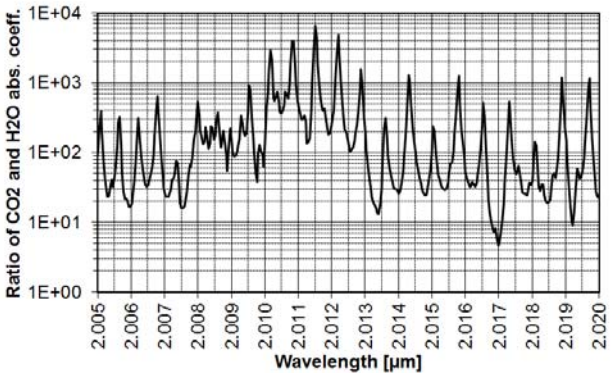

Fig. 14. Ratio between the absorption coefficients of CO_2 and H_2O (1 atm, 296 K) from 2005 to 2020 nm [10].

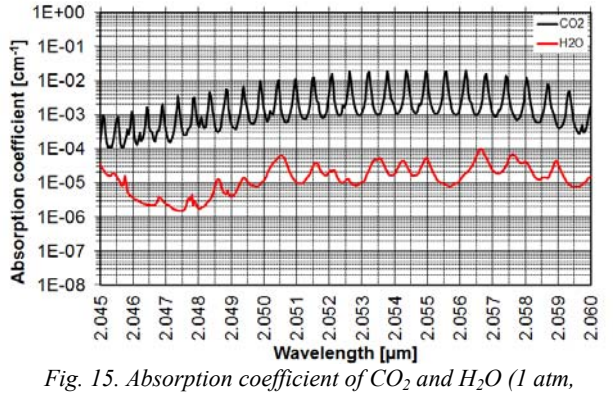

Fig. 15. Absorption coefficient of CO_2 and H_2O (1 atm, 296 K) from 2045 to 2060 nm [10].

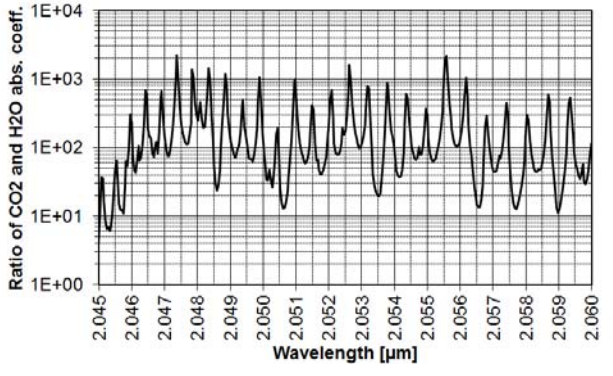

Fig. 16. Ratio between the absorption coefficients of CO_2 and H_2O (1 atm, 296 K) from 2045 to 2060 nm [10].

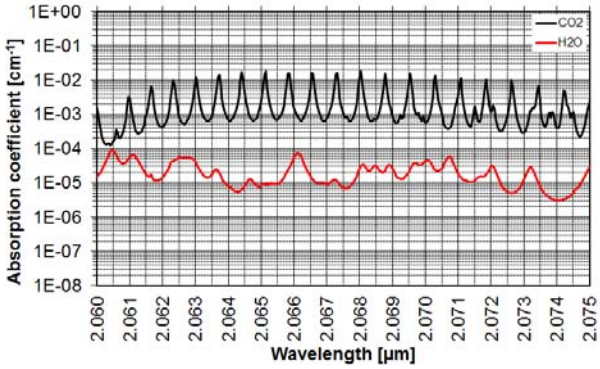

Fig. 17. Absorption coefficient of CO_2 and H_2O (1 atm, 296 K) from 2060 to 2075 nm [10].

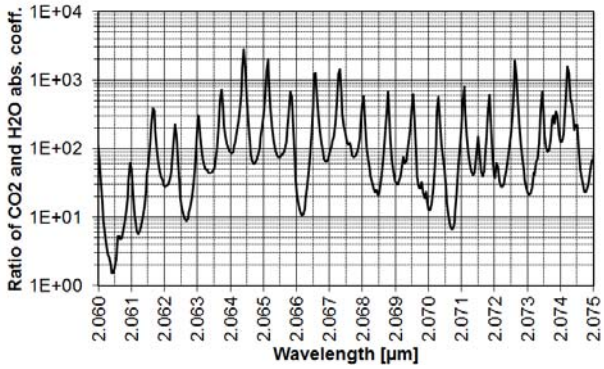

Fig. 18. Ratio between the absorption coefficients of CO_2 and H_2O (1 atm, 296 K) from 2060 to 2075 nm [10].

Table 2. λ_{ON} candidates for DIAL measurement of carbon dioxide in volcanic plumes.

Spectral window	λ_{ON} [nm]	λ_{ON} [cm^{-1}]	CO_2 abs. coeff. [cm^{-1}]	Ratio between CO_2 and H_2O abs. coeff.	Ratio between CO_2 abs. coeff. and its max. in the sp. win.
1570-1585 nm	**1572.6**	**6358.7**	**1.14E-03**	**3.3E+03**	**85%**
	1577.4	6339.7	1.02E-03	3.1E+03	76%
	1582.0	6321.2	7.29E-04	2.9E+03	54%
1600-1615 nm	1600.4	6248.6	8.12E-04	7.8E+03	59%
	1603.2	**6237.4**	**1.21E-03**	**7.1E+03**	**88%**
	1612.0	6203.4	8.72E-04	6.9E+03	64%
2005-2020 nm	2010.9	4973.0	4.40E-02	3.9E+03	47%
	2011.5	4971.4	6.31E-02	6.5E+03	68%
	2012.2	**4969.7**	**7.50E-02**	**4.8E+03**	**80%**
2045-2060 nm	2047.4	4884.3	3.46E-03	2.3E+03	17%
	2052.6	4871.8	1.86E-02	1.6E+03	92%
	2055.6	**4864.8**	**1.86E-02**	**2.2E+03**	**92%**
2060-2075 nm	**2064.4**	**4844.0**	**1.76E-02**	**2.8E+03**	**99%**
	2065.1	4842.3	1.77E-02	1.9E+03	100%
	2072.6	4824.8	9.62E-03	1.9E+03	54%

If one compares the three peaks with largest ratio between the absorption coefficients of CO_2 and H_2O in the above mentioned five spectral windows, fifteen candidates for λ_{ON} can be selected (Table 2). In each spectral window, the peak with largest CO_2 absorption coefficient has been regarded as more promising and has been written in bold.

Typical fixed-wavelength lasers cover only one spectral window: fiber lasers emit at around 1573 nm and Tm,Ho:YLF lasers emit at around 2051 nm. It would be desirable to have a tunable laser covering all the five spectral windows for the following reasons:

1. the CO_2 absorption coefficient would span from about 1E-03 to 1E-01 cm^{-1}, allowing one to choose the absorption coefficient that fits more the measurement scenario (trade-off between accuracy and range);
2. both the spectral regions around 1.6 and 2.05 µm would be reachable (each one of them has advantages: at 1.6 µm the best detectors are available while at 2.05 µm the CO_2 absorption coefficient is larger);
3. it would be easier to choose λ_{OFF} so that the H_2O absorption coefficient at λ_{ON} and λ_{OFF} is nearly the same, thus minimizing the cross sensitivity of the lidar measurement to H_2O.

Both fixed-wavelength and tunable lasers should be:

1. narrow band;
2. low divergence;
3. short pulse.

The atmospheric absorption coefficient at seven altitudes around 1.57 and 2.07 µm is shown in Fig. 19 and Fig. 20, respectively. The strong lines are due to CO_2. Increasing the altitude, the lines narrow. The bandwidth of the CO_2 absorption lines is given in Table 3. Taking into account that our measurement will likely be below 3 km, the laser bandwidth should be < 0.05 cm^{-1}, i.e. < 12 pm for the 1.57 µm region and < 20 pm for the 2.07 µm region.

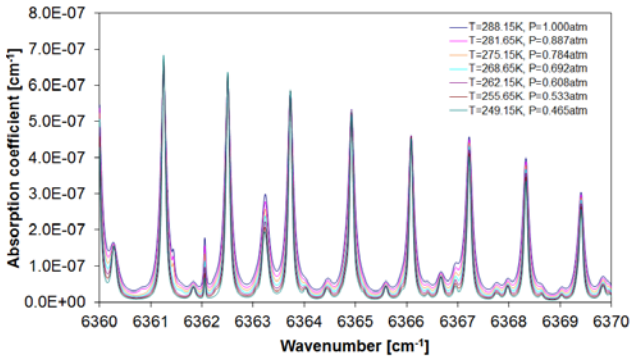

Fig. 19. Atmospheric absorption coefficient (Mid Latitude Summer Model of the United States Standard Atmosphere [14]) around 1.57 µm at seven altitudes (see Table 3).

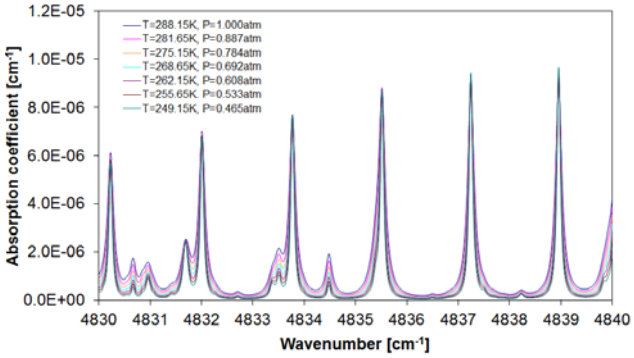

Fig. 20. Atmospheric absorption coefficient (Mid Latitude Summer Model of the United States Standard Atmosphere [14]) around 2.07 µm at seven altitudes (see Table 3).

Table 3. Bandwidth of the CO_2 absorption lines at different altitudes (Mid Latitude Summer Model of the United States Standard Atmosphere [14]).

Altitude [km]	Temperature [K]	Pressure [atm]	Δλ @ 1.6 µm [cm^{-1}]	Δλ @ 2.05 µm [cm^{-1}]
0	288.15	1	0.164	0.164
1	281.65	0.887	0.146	0.146
2	275.15	0.784	0.132	0.130
3	268.65	0.692	0.118	0.118
4	262.15	0.608	0.105	0.104
5	255.65	0.533	0.096	0.094
6	249.15	0.465	0.086	0.084

For typical telescope focal lengths (~1 m) and detector sizes (~0.5 mm) a beam full angle divergence less than 0.5 mrad would be highly desirable.

A pulse duration shorter than 100 ns would lead to a 15-m range resolution, adequate to our purposes.

5. Conclusions

DIAL measurement of carbon dioxide in volcanic emissions should be performed in the 1.6 or 2.05 µm bands. After examining the absorption coefficient of carbon dioxide and water vapor, five spectral windows have been retained: 1570-1585 nm, 1600-1615 nm, 2005-2020 nm, 2045-2060 nm and 2060-2075 nm. Eventually, one wavelength per spectral window has been selected for DIAL measurement of carbon dioxide (in bold in Table 2), having in mind to reduce cross sensitivity to water vapor.

The observation of the atmospheric absorption coefficient at different altitudes led to the conclusion that laser transmitter should have a linewidth narrower than 0.05 cm^{-1}.

Beam full angle divergence and pulse duration should be less than 0.5 mrad and 100 ns, respectively, in order to accurately profile volcanic plumes.

Acknowledgements

The authors are deeply grateful to R. Fantoni and A. Palucci for constant encouragement. W. Saleh gratefully acknowledges the hospitality of ENEA and the support of the Abdus Salam International Centre for Theoretical Physics (ICTP) in the framework of the program Training and Research in Italian Laboratories (TRIL). The support from the European Research Council project CO2VOLC, grant agreement no. 279802, is gratefully acknowledged.

References

[1] D. Sakaizawa, C. Nagasawa, T. Nagai, M. Abo, Y. Shibata, M. Nakazato, T. Sakai, Appl. Opt. **48**, 784 (2009).

[2] G. J. Koch, J. Y. Beyon, F. Gibert, B. W. Barnes, S. Ismail, M. Petros, P. J. Petzar, J. Yu, E. A. Modlin, K. J. Davis, U. N. Singh, Appl. Opt. **47**, 944 (2008).

[3] L. Fiorani, in Progress in Laser and Electro-Optics Research, V. V. Koslovskiy, ed., 21-75 (Nova, New York, 2010).

[4] European Research Council project n. 279802, CO2VOLC: Quantifying the global volcanic CO_2 cycle.

[5] L. Fiorani, F. Colao, A. Palucci, Opt. Lett. **34**, 800 (2009).

[6] P. Weibring, H. Edner, S. Svanberg, G. Cecchi, L. Pantani, R. Ferrara, T. Caltabiano, Appl. Phys. B **67**, 419 (1998).

[7] L. Fiorani, F. Colao, A. Palucci, D. Poreh, A. Aiuppa, G. Giudice, Opt. Comm. **284**, 1295 (2011).
[8] P. J. Linstrom W. G. Mallard, eds., NIST Chemistry WebBook, http://webbook.nist.gov (National Institute of Standards and Technology, Gaithersburg, retrieved June 18, 2012).
[9] R. T. Menzies, D. M. Tratt, Appl. Opt. **42**, 6569 (2003).
[10] L. S. Rothman, I. E. Gordon, A. Barbe, D. C. Benner, P. F. Bernath, M. Birk, V. Boudon, L. R. Brown, A. Campargue, J.-P. Champion, K. Chance, L. H. Coudert, V. Dana, V. M. Devi, S. Fally, J.-M. Flaud, R. R. Gamache, A. Goldman, D. Jacquemart, I. Kleiner, N. Lacome, W. J. Lafferty, J.-Y. Mandin, S. T. Massie, S. N. Mikhailenko, C. E. Miller, N. Moazzen-Ahmadi, O. V. Naumenko, A. V. Nikitin, J. Orphal, V. I. Perevalov, A. Perrin, A. Predoi-Cross, C. P. Rinsland, M. Rotger, M. Šimečková, M. A. H. Smith, K. Sung, S. A. Tashkun, J. Tennyson, R. A. Toth, A. C. Vandaele, J. VanderAuwera, J. Quant. Spectrosc. Radiat. Transfer **110**, 533 (2009).
[11] F. Gibert, P. H. Flamant, J. Cuesta, D. Bruneau, J. Atm. Ocean. Tech. **25**, 1478 (2008).
[12] G. J. Koch, J. Y. Beyon, F. Gibert, B. W. Barnes, S. Ismail. M. Petros, P. J. Petzar, J. Yu, E. A. Modlin, K. J. Davis, U. N. Singh, Appl. Opt. **47**, 944 (2008).
[13] D. N. Whiteman, K. Rush, I. Veselovskii, M. Cadirola, J. Comer, J. R. Potter, R. Tola, J. Atm. Ocean. Tech. **24**, 1377 (2007).
[14] Committee on Extension to the Standard Atmosphere, United States Standard Atmosphere, United States Government Printing Office, Washington (1976)

*Corresponding author: luca.fiorani@enea.it